# ION DEBRIS AND X-RAY ENERGY DEPOSITION AND RESPONSE OF FUSION REACTOR FIRST WALLS*

A.M. HASSANEIN

*Fusion Power Program, Argonne National Laboratory, Argonne, IL 60439-4837, USA*

H.M. ATTAYA, and G.L. KULCINSKI

*Nuclear Engineering Department, University of Wisconsin, Madison, WI 53706, USA*

The energy deposition of the thermonuclear target explosion products in Inertial Confinement Fusion (ICF) reactors, i.e., ion debris and X-rays and the resulting thermal response of first wall materials, is calculated using the computer code ATEN. Models to accurately simulate the ion and X-ray energy deposition and the consequent response of the wall are implemented in the code. Simultaneous multiple ions and X-rays with different yields and spectra incident on various wall materials are easily handled by the code. In a laser driven ICF reactor, in addition to X-rays, ions, and neutrons, the first wall will be exposed to the portion of the laser light reflected from the target. This could have an important effect on the overall performance of the wall.

The thermal response and the resulting melting and erosion due to vaporization of wall materials are found to be critically dependent on target design configuration. Depending on the details of target design, its constituents and the driver beam, a wide range of X-ray and ion debris yields and spectra can be generated as a result of the thermonuclear reaction. A parametric study of first wall temperature excursion, resulting melt thickness and material loss for different candidate wall materials is presented. It is found that controlling the partition between X-ray energy yield and ion energy yield and their spectra can substantially result in a longer first wall lifetime for the same total target yield.

## 1. Introduction

The protection of cavity surface components in an ICF reactor from damage due to different radiation types, i.e., neutrons, target debris and X-rays released from the thermonuclear burn, is a key requirement for the successful operation of the reactor. The high energy neutrons carrying about 75% of the total energy released will pass through the first wall without depositing any significant amount of this energy. The rest of the energy released from the burn will be in the form of charged particles and X-rays. The ion debris energy will be absorbed in the first few microns of the wall. Depending on both energy spectrum of the X-rays as well as on the wall material, the absorption of the X-ray energy will range from a few microns to a few millimeters [1,2]. By designing the target with high density–radius ($\varrho R$) product some of the neutron energy will be deposited in the target debris which increases the fraction of the total energy released in the form of charged particles and X-rays [3].

The partition of the energy between X-rays and target debris depends on the target design as well as on the energy source driving the thermonuclear burn [3]. The deposition of X-ray and ion debris energy is a short distance within the first walls and in a very short time will result in very high surface temperatures which may cause melting and evaporation that can limit the reactor performance.

The computer code ATEN [4], a combined and enhanced version of both the A*THERMAL [5] and T-DAMEN [6] computer codes, is designed to calculate the response of a fusion reactor first wall by analytical and numerical techniques for any kind of incident radiation energy deposition. These energy depositions include simultaneous combinations of several energetic ions with different spectra and energy ranges, X-ray energy with different spectra and characteristic temperatures, and any reflected laser light with various wave lengths. These incident radiations in the first wall of an ICF reactor differ substantially in their time duration and spatial extent. The code sums the energy deposited from all the radiations and stores it in a single time–space grid. This grid has a variable mesh interval in both time and space. It also verifies the energy balance and readjusts the mesh intervals accordingly.

The code solves the heat conduction equation by numerical and analytical methods with temperature variable thermal properties, and uses the surface temperature to compute the evaporation rate. Moving boundary conditions are included for both surface recession from evaporation and solid-liquid interface during possible change of phase [7]. The Green's function method can be used for a quick estimate of the temperature rise and evaporation rate [8]. The code also contains several models for calculating the energy deposited into the wall from different kinds of radiations.

One main purpose of this paper is to use the code to study the effect of the energy partition between ions and X-rays on the wall thermal response and erosion rate. The sensitivity of the wall thermal response to the uncertainty due to X-ray and ion spectra and their de-

position time is also studied for both carbon and silicon carbide as potential candidate wall materials.

## 2. Thermal response of carbon and silicon carbide first walls

### 2.1. Incident radiation spectra

The purpose of this study is not to design a reactor first wall with a successful operation. It is only intended to realistically simulate the response of unprotected first wall exposed to different radiation spectra and to explore the important factors that can have the most effect on the wall thermal response. The X-ray and ion spectra for the reference case used in these calculations are taken from SIRIUS [9] reactor design. These spectra are shown in fig. 1. The ion spectra are assumed to have a very narrow Gaussian spectra (almost monoenergetic) and their mean characteristic energy and to-
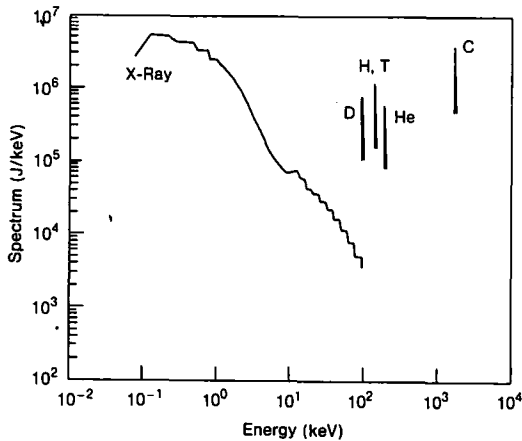


Fig. 1. Reference case X-ray and ion spectra.

tal number of ions are listed in table 1. The X-ray spectrum extends from a very soft component (0.1 keV) up to much harder value (100 keV). In addition to X-rays and ions, the first wall is exposed to a laser light reflected from the target [9]. This reflected light is assumed to be uniformally distributed over the entire wall. The reflected portion from one location off the wall is assumed to strike the opposite side in a train series of laser pulses with rapidly attenuated amplitudes. The total energy content in both the ions and X-rays are 26 MJ and 8 MJ respectively. About 10% of the laser energy (i.e., 0.1 MJ) is assumed reflected from the target and ultimately absorbed by the wall. In this study the reactor cavity is assumed to be spherically symmetric with a radius of 9 m and an ambient wall temperature of 500 K.

### 2.2. Wall thermal response

The temperature rise as a function of time for both carbon and silicon carbide resulting from X-ray and ion energy deposition is shown in fig. 2. The X-ray deposition time for this case is assumed to be 20 ps (20 × $10^{-12}$ s), i.e., of the order of the thermonuclear burn time. The first peak in the temperature rise is mainly due to X-rays while the other peaks are mainly due to the ions. It can be seen that the temperature rise due to X-rays is much lower in C than in SiC. This is because the lower atomic number materials (i.e., lower X-ray absorption cross-section) filter out the low temperature components of the spectrum and spread the energy deposited over a larger volume leading to a lower specific energy density [1,2]. This has the effect of reducing the surface temperature and consequently reducing the erosion rate due to vaporization. Although the carbon has a much lower maximum temperature rise, its temperature in between the deposition pulses

Table 1
Reference case for ion and X-ray spectra used in the calculations

| Density–radius product ($\varrho R$) | | = 1.3 g/cm$^2$ |
| Total ions energy content | | = 26 MJ |
| Total X-ray energy | | = 8 MJ |
| X-ray deposition time | | = 20 ps |

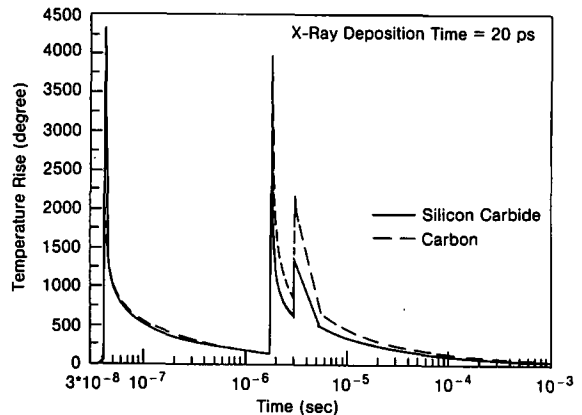| Ion | Gaussian mean energy and spread (keV) | No. of ions (× $10^{20}$) | Energy content (MJ) |
|-----|------|------|------|
| H | 137.5 ± 1 | 1.30 | 2.88 |
| D | 92.5 ± 1 | 1.20 | 1.80 |
| T | 139.0 ± 1 | 1.20 · | 2.70 |
| He | 185.0 ± 1 | 0.47 | 1.38 |
| C | 1649.0 ± 2 | 0.65 | 17.25 |



Fig. 2. Surface temperature rise for silicon carbide and carbon for the reference spectra.

remains higher than SiC most of the time especially at the longer time domain where it has the most effect on the evaporation as will be seen later. One reason for this is the lower thermal conductivity of carbon at higher temperatures that prevents the temperature from dropping as rapidly as SiC.

The effect of the energy partition between ions and X-rays on the total evaporation rate calculated in mm/ fpy (millimeter per full power year) of carbon and SiC assuming one thermonuclear burn per second (i.e., 1 Hz) is shown in fig. 3. The X-ray energy content is varied from 10% to 60% of the fixed total yield of 34 MJ. The arrow in the figure points to the reference case listed in table 1 where the X-rays contain 8 MJ while the ions have 26 MJ. As the fraction of X-ray energy content increases, the evaporation rate decreases until it comes to a minimum and then it increases again. This is primarily because for smaller fractions of the total yield in X-rays the evaporation is mainly due to the ions which contain the larger fraction of the total yield. As the fraction of the X-ray energy content becomes very large, the evaporation is entirely determined by the temperature rise due to the X-ray energy deposition. The carbon evaporation rate is more than an order of magnitude higher than that for SiC at X-ray energy fractions of 25% of the total yield or less. This is despite the much lower maximum surface temperature of carbon compared to SiC (as shown in fig. 1 for the reference case). However, for larger fractions of the X-ray energy content the carbon evaporation is much less than that for SiC. This is primarily because the X-ray absorption cross-section of carbon (lower
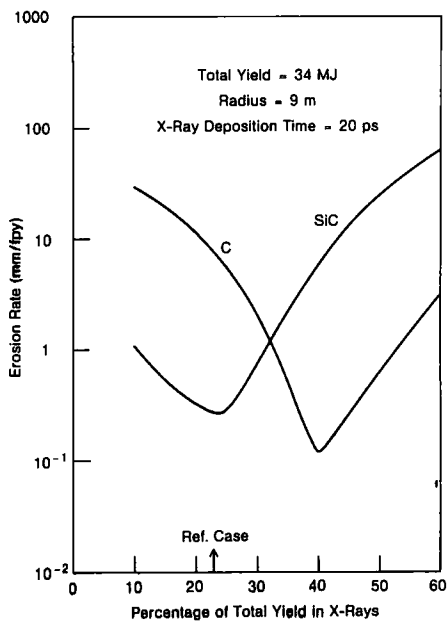
atomic number) is much less than SiC absorption cross-sections.

Another important factor in determining the wall response is the X-ray energy deposition time. This time can vary from a few pico-seconds, i.e., the burn time [9] up to a few nano-seconds [10], depending on the target design and the dynamics of the thermonuclear burn. Fig. 4 shows the temperature distribution for the reference case of X-rays and ions spectra shown in fig. 1 except the X-ray deposition time is assumed to be 20 ns. It can be seen that the large temperature excursion previously shown in fig. 2 due to the X-ray deposition pulse is almost eliminated as the deposition time is increased. This has a significant effect on the total amount of erosion from surface vaporization due to the X-ray deposition as shown in fig. 5. The conditions in this figure are similar to those in fig. 3 except for the deposition time of X-rays. However in this case, increasing the fraction of X-ray energy content will decrease the total evaporation rate. This is mainly because most of the evaporation is due to the ions and as their fraction of the energy content decreases the evaporation rate also decreases. The calculation is also done for X-ray energy deposition time of 2 ns. It is found that the temperature rise due to X-rays is still much lower than the ion temperature rise especially for SiC where the X-rays have more impact than for carbon since SiC has a much higher absorption cross-section for X-rays.

The X-ray energy spectrum itself can also have a significant effect on the wall thermal response. Depending on the details of target design, constituents, and the driver beam, a wide range of X-ray spectra are possible from the fusion target micro-explosions. Fig. 6 shows the X-ray evaporation rate as a function of the blackbody temperature for X-ray total energy of 17 MJ (50% of the reference case's total yield) and deposition time of 20 ps. The blackbody spectrum is commonly



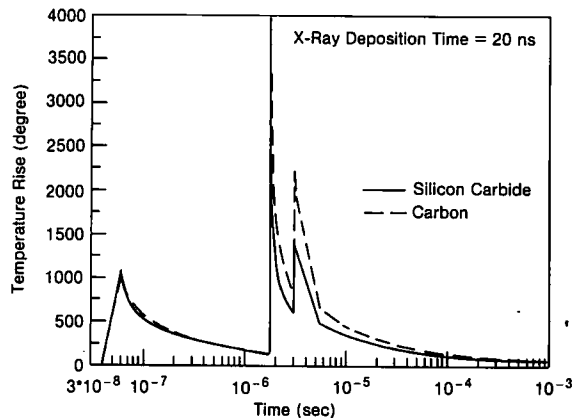Fig. 3. Evaporation rate as a function of the percentage of the total yield in X-rays.



Fig. 4. Surface temperature rise for silicon carbide and carbon for 20 ns X-ray deposition time.

used for low energy photons where the radiation emitted is specified by the temperature of the emitter [11]. As can be seen from fig. 6, the evaporation rate sharply decreases as the blackbody temperature increases (i.e., harder spectra) even at this very short deposition time. Very soft spectra (low blackbody temperatures) are absorbed very near the surface layer which increases the surface temperature and accordingly the resulting evaporation. X-ray spectra from structured targets containing high atomic number materials are expected to have
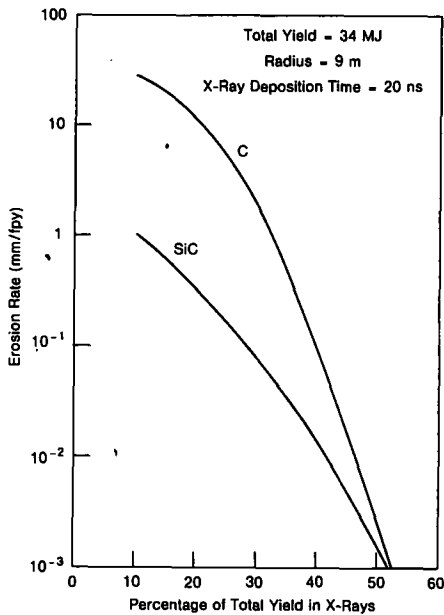


Fig. 5. Evaporation rates as a function of the percentage of the total yield in X-rays deposited in 20 ns.
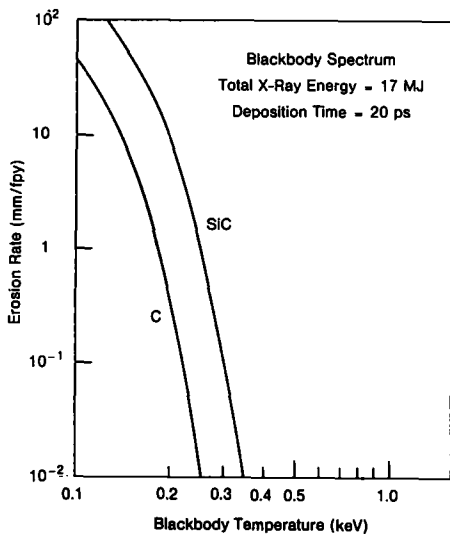


Fig. 6. Evaporation rate from blackbody X-ray spectra as a function of blackbody temperature.

a blackbody distribution. The blackbody temperature will depend on the yield, mass and composition of the target [12].

The ions spectra can also have a wide range of distributions depending on the dynamics of the implosion and on the interactions of different species in the target constituents as well as on the target structure itself. To show the effect of different spectra on the temperature rise and on the resulting evaporation, it is assumed that the ions have a Maxwellian energy distribution, as shown in fig. 7, with the same total energy content as that of the reference narrow Gaussian distribution. Figs. 8 and 9 show the temperature rise for the reference case and for the Maxwellian case for both carbon and SiC respectively. The Maxwellian distribution of the ions yields a much lower surface temperature than the reference case and the total evaporation rate is calculated to be more than five orders of magnitude lower. Fig. 9 also shows the large difference in the X-ray tem-
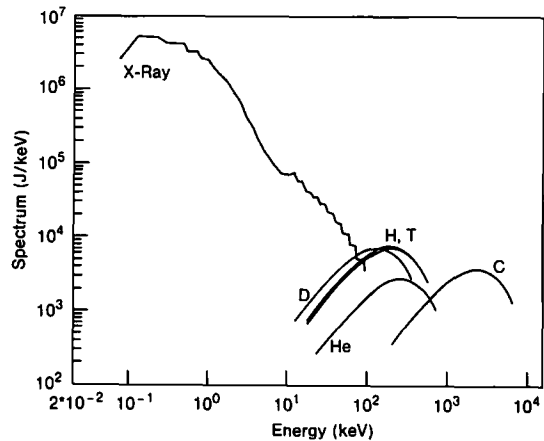


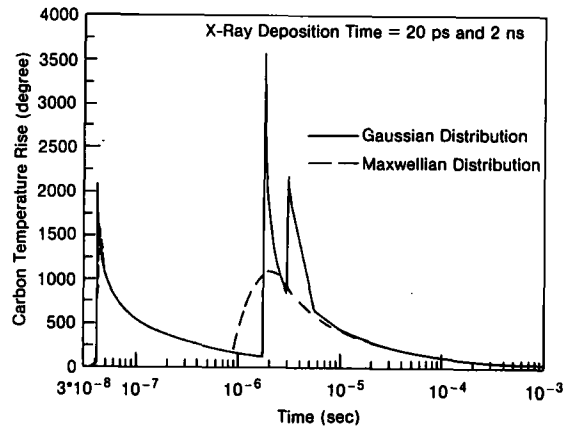Fig. 7. X-ray and Maxwellian ion energy spectra.



Fig. 8. Surface temperature rise of carbon for the reference case spectra but with Maxwellian's ion spectra distribution.
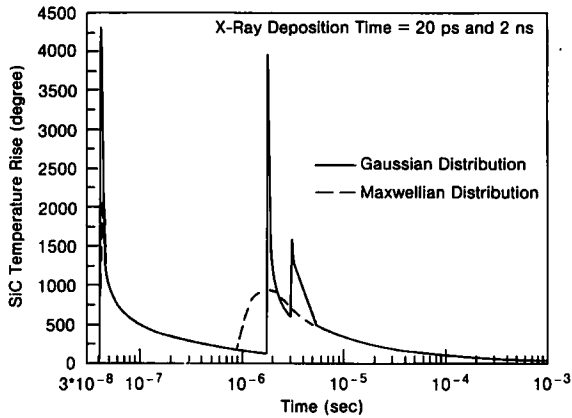
Fig. 9. Surface temperature rise of SiC for different ion spectra and different X-ray deposition time.

perature rise (first peak) in SiC between deposition times of 20 ps and 2 ns as mentioned previously.

## Conclusions

The parametric study of the first wall erosion from surface evaporation due to X-ray and ion energy deposition in ICF reactors shows that controlling the partition in energy between X-rays and ions can greatly reduce the temperature excursion resulting from the thermonuclear burn. The X-ray and ion deposition time and their energy spectra can be very important parameters in reducing the surface evaporation rate. Longer deposition times in both X-rays and ions for the same total energy deposited produce lower surface temperatures. Harder X-ray spectra are deposited over a larger

volume inside the material which reduces the temperature rise. Lower atomic number materials filter out the low energy components of the X-ray spectrum which also helps to spread the energy deposited inside the material leading to better wall protection. In general, a better understanding of the physics of implosion and target design in controlling the partition in ion debris and X-ray energy and their overall spectra can lead to a much easier protection of the reactor cavity. This can significantly prolong the wall lifetime without using complicated methods of protecting the cavity walls.

## References

[1] A.M. Hassanein, J. Nucl. Mater. 122–123 (1984) 1459.

[2] A.M. Hassanein et al., J. Nucl. Mater. 103–104 (1981) 327.

[3] J.A. Blink et al., Trans. ANS 1977 Winter Meeting, San Francisco, CA (1977) 70.

[4] H.M. Attaya, University of Wisconsin Fusion Technology Institute Report, to be published.

[5] A.M. Hassanein, Ph.D Thesis, University of Wisconsin UWFDM-465 (1982).

[6] T.O. Hunter and G.L. Kulcinski, University of Wisconsin UWFDM-247 (1978).

[7] A.M. Hassanein et al., Nucl. Engr. Design/Fusion 1 (1984) 307.

[8] A.M. Hassanein and G.L. Kulcinski, J. Heat Transfer 106 (1984) 486.

[9] B. Badger et al., University of Wisconsin Fusion Technology Institute Report UWFDM-568 (March 1984).

[10] B. Badger et al., A Joint Federal Republic of Germany–University of Wisconsin, UWFDM–450 (1981).

[11] E.U. Condon and H.O. Dishaw, eds., Handbook of Physics 2nd ed. (McGraw-Hill, New York, 1957) p. 7.

[12] T.G. Frank et al., AICHE Symposium Series 73, No. 168 (1976) 77.